MOLECULAR AND CELLULAR BIOLOGY, Sept. 2006, p. 6656–6663 Vol. 26, No. 17
0270-7306/06/$08.00+0 doi:10.1128/MCB.00091-06

Loss of the Mouse Ortholog of the Shwachman-Diamond Syndrome Gene (*Sbds*) Results in Early Embryonic Lethality†

Siyi Zhang,[1,2] Mingjun Shi,[2] Chi-chung Hui,[1,3] and Johanna M. Rommens[1,2]*

Department of Molecular and Medical Genetics, University of Toronto,[1] and Programs in Genetics and Genomic Biology[2] and Developmental Biology,[3] Research Institute, The Hospital for Sick Children, Toronto, Canada

Received 15 January 2006/Returned for modification 18 February 2006/Accepted 5 June 2006

Mutations in *SBDS* are responsible for Shwachman-Diamond syndrome (SDS), a disorder with clinical features of exocrine pancreatic insufficiency, bone marrow failure, and skeletal abnormalities. SBDS is a highly conserved protein whose function remains largely unknown. We identified and investigated the expression pattern of the murine ortholog. Variation in levels was observed, but Sbds was found to be expressed in all embryonic stages and most adult tissues. Higher expression levels were associated with rapid proliferation. A targeted disruption of *Sbds* was generated in order to understand the consequences of its loss in an in vivo model. Consistent with recessive disease inheritance for SDS, *Sbds*$^{+/-}$ mice have normal phenotypes, indistinguishable from those of their wild-type littermates. However, the development of *Sbds*$^{-/-}$ embryos arrests prior to embryonic day 6.5, with muted epiblast formation leading to early lethality. This finding is consistent with the absence of patients who are homozygous for early truncating mutations. *Sbds* is an essential gene for early mammalian development, with an expression pattern consistent with a critical role in cell proliferation.

Shwachman-Diamond syndrome (SDS) (OMIM entry 260400) is a rare autosomal recessive disorder with major clinical features, including exocrine pancreatic insufficiency, bone marrow failure, and skeletal abnormalities (4, 29). Patients present with failure to thrive, susceptibility to infections, and short stature. Deficiency in the pancreas manifests as early as the postnatal period, with sparse numbers of pancreatic acinar cells. Exocrine components are replaced by fatty tissue, while the islets of Langerhans and the ductal architecture appear intact. Low levels of trypsinogen, amylase, lipase, and other exocrine proteins consequently impair digestive function (1, 13, 14). During childhood, up to 50% of SDS patients show modest improvement in enzyme production and can become pancreatically sufficient with normal fat absorption (18). The bone marrow failure manifests with intermittent deficiency of myeloid lineages including anemia with low reticulocyte levels and thrombocytopenia or, most frequently, neutropenia. It has been suggested that stem cell and, probably, stromal cell defects contribute to insufficient cell numbers in myeloid lineages (1, 10). Neutropenia occurs in 88 to 98% of patients and has been identified as early as the neonatal period (1, 10). Patients are susceptible to recurrent infections, and adding to this risk have been indications of impaired neutrophil chemotactic functions (2, 9, 31). Bone marrow biopsy usually reveals varying degrees of hypoplasia and fat infiltration. A significant proportion of patients develop pancytopenia and myelodysplasia, and it has been estimated that up to one-third of studied SDS patients develop leukemia, mostly acute myeloid leukemia (8, 30, 32). SDS is considered an important model for understanding the molecular mechanisms involved in the progression to leukemia.

Another prominent phenotype of SDS, the skeletal dysplasia, appears to be the result of delayed bone maturation. Typical clinical aspects include short statue, delayed appearance of secondary ossification centers, and generalized osteopenia, with variable widening and irregularity of the metaphyses in early childhood followed by progressive thickening and irregularity of the growth plates (19). Additional features include early liver biochemical disturbances as well as some behavioral and learning features that remain poorly defined (1, 10, 15, 17).

Previously, we have identified SDS-associated loss-of-function mutations in a novel gene on chromosome 7q11, designated *SBDS* (5). Recurring mutations arise from conversion between *SBDS* and its highly similar pseudogene, *SBDSP*. Extensive genotype-phenotype correlation has not been reported for SDS, although there is an absence of patients with a combination of early truncating alterations (5; N. Richards et al., unpublished data).

Analysis of the sequence of SBDS with 250 amino acids reveals membership in a highly conserved protein family with orthologs in all sequenced archaea and eukaryotes, but it is absent in prokaryotes (5, 6). Limited functional information exists, although the structure of the *Archaeoglobus fulgidus* SBDS ortholog (accession no. AF0491) was recently solved, revealing a three-domain architecture: a novel fold of the N-terminal domain, a common winged helix-turn-helix central domain, and a ferredoxin-like C-terminal domain which occurs in some DNA and RNA binding proteins (27, 28).

Consistent with its phylogeny, additional indirect evidence supports a role for SBDS in RNA metabolism and/or ribosome biogenesis (6). The yeast ortholog, YLR022c, is an essential gene and is clustered with RNA-processing enzymes on the basis of microarray expression profile analysis in yeast (25, 33). The archaeal orthologs are located in highly conserved superoperons containing a number of genes, including those in-

* Corresponding author. Mailing address: Research Institute, Program in Genetics and Genomic Biology, Room 15-313 TMDT, 101 College Street, East Tower, Toronto, Ontario M5G 1L7, Canada. Phone: (416) 813-7095. Fax: (416) 813-4931. E-mail: jrommens@sickkids.ca.

† Supplemental material for this article may be found at http://mcb.asm.org/.

volved with RNA processing, e.g., orthologs of the eukaryotic exosome and RNase P complex subunit genes (16). The predicted protein products of plant orthologs appear to have an additional C-terminal domain containing an RNA binding U1-type zinc finger.

Understanding the pathobiology of SDS has been challenging even with the recent molecular findings because of the absence of adequate information on gene expression. Further, the high variability in disease presentation together with the manifestation of severe disease phenotypes in a combination of organs not commonly seen in other bone marrow failure syndromes have confounded interpretations of genotype-phenotype correlations in patients. In this study, we pursued the mouse as a model and found that the *SBDS* ortholog has a ubiquitous, but variable, expression pattern during embryonic development and in adult tissues. Increased expression was found in rapidly proliferating cells. Ablation of Sbds results in early embryonic lethality in the homozygote with failure of epiblast development.

MATERIALS AND METHODS

Northern blot analysis. Mouse multiple tissue and embryo RNA blots (Clontech) were hybridized with a ^{32}P-labeled cDNA probe including the entire open reading frame of *Sbds*, using standard methods (26). The blots were subsequently stripped and hybridized with a ^{32}P-labeled mouse *Gapd* cDNA probe to evaluate the integrity and loading of RNA.

Western blot analysis. A polyclonal antibody generated against recombinant full-length human SBDS was affinity purified using a Sepharose column with immobilized protein A (Sigma). The specificity of the anti-SBDS rabbit polyclonal antibody was initially confirmed for Western blotting with epitope-tagged SBDS expressed in heterologous cells (see Fig. S1 in the supplemental material). CD-1 mouse (Charles River Labs; 6 weeks of age) protein extracts from liver, brain, heart, spleen, pancreas, kidney, lung, testis, and skeletal muscle tissues were prepared as follows. Approximately 100 mg of tissue was homogenized in lysis buffer (50 mM Tris [pH 8.0], 150 mM NaCl, 1% Triton X-100, 0.5% sodium deoxycholate, and 0.1% sodium dodecyl sulfate) supplemented with proteinase inhibitor cocktail (Roche). Bone marrow protein extract was prepared from flushed bone marrow cells of adult CD-1 mouse femurs with 1× phosphate-buffered saline (PBS) buffer. All homogenized lysates were centrifuged at 10,000 × *g* for 15 min to remove insoluble material. Proteins (30 μg in each lane) were separated by electrophoresis using 12.5% sodium dodecyl sulfate-polyacrylamide gels and transferred by electroblotting to Hybond-C membrane (Amersham Bioscience). The blots were initially blocked overnight with TBST buffer (10 mM Tris-HCl [pH 7.5], 150 mM NaCl, 0.05% Tween 20) containing 5% milk powder and incubated with rabbit anti-SBDS (1:2,000 in blocking solution) for 4 h. The blots were then washed four times in TBST (5 min per wash), incubated with a horseradish peroxidase-conjugated anti-rabbit immunoglobulin G (1:3,000 in blocking solution) (Bio-Rad), and washed three times with TBST (10 min per wash). Signals were visualized using the enhanced chemiluminescence (ECL; Pharmacia) technique with BioMax MR X-ray film (Kodak).

Tissue section preparation. Mouse tissues and deciduae at embryonic stages were fixed overnight in 4% paraformaldehyde in 1× PBS buffer (pH 7.3), washed twice for 30 min each in 1× PBS buffer (pH 7.3) at 4°C, dehydrated, and embedded in paraffin. Paraffin blocks were sectioned as 7-μm slices for histology, immunohistochemistry, and in situ hybridization analyses.

In situ hybridization analysis. To investigate the expression of *Sbds* in mouse embryo and adult mouse tissue, a cDNA probe covering the 5′ untranslated region (UTR) and exons 1 through 3 of *Sbds* was prepared by reverse transcription-PCR (RT-PCR) amplification of mouse liver total RNA with oligonucleotide primers S1 (5′CTGGCTAGTGCGCCACTTGA) and S2 (5′CAGCTGTG TGTGCCGTTCTT). To verify the absence of *Sbds* expression in the null embryo, a cDNA probe covering exons 3 and 4 was prepared by RT-PCR amplification from mouse liver total RNA with primers S3 (5′CACACACAGC TGGAGCAGAT) and S4 (5′AGCTGCTGGCTGTAGTCCTC). The corresponding fragments were inserted into the pDrive vector (QIAGEN) as per the supplier's protocols. In situ hybridizations with digoxigenin-labeled antisense and sense probes were carried out on paraffin sections as described previously (21, 23).

Generation of *Sbds*-targeted mice. An *Sbds* cDNA probe was used to screen the RPCI-22 bacterial artificial chromosome (BAC) library constructed from the 129S6/SvEvTac mouse strain with the facilities of The Center for Applied Genomics at The Hospital for Sick Children. One of the positive BAC clones, 138L15, was found to contain the intact genomic sequence of *Sbds*. Isolated DNA was digested with XbaI to isolate an 11.7-kb DNA fragment containing an upstream segment (5.2 kb) as well as exons 1 through 3. The fragment was recloned into pBluescript vector (Stratagene) and was subsequently digested with BssSI and XbaI to isolate an 8.5-kb subfragment containing only 1 kb of the upstream region and exons 1 to 3. The fragment ends were filled in for cloning into the PGKneolox2DTA vector (a gift of the Soriano Lab, Fred Hutchinson Cancer Research Center, Seattle, WA) by using the XbaI and EcoRI sites. The vector contained the diphtheria toxin A gene as a negative selection marker. The positive selection marker cassette containing the *IRES-lacZ* fusion gene and the neomycin resistance gene under control of a mouse phosphoglycerate kinase promoter was inserted into the Eco47III site of exon 1 to disrupt the translation of *Sbds*. The vector was linearized with NotI and electroporated into W4 embryonic stem (ES) cells (Taconic) by InGenious Targeting Laboratory, Inc. A total of 288 G418-resistant clones were screened by Southern analysis using two distinct mouse genomic probes external to the vector segments. Sixty-eight clones were found to be correctly targeted. Two clones were further verified to have a single gene site insertion with a neomycin resistance gene fragment probe. Male chimeras were generated by injection of two independent ES clones into C57BL/6J blastocysts, and germ line transmission was verified by Southern analysis. *Sbds* heterozygotes were intercrossed to generate homozygous mutants.

Genotyping analysis. Genotyping of mice was carried out by PCR using three oligonucleotide primers: a common primer located in the first intron (primer c, 5′CTGGGCACAGGATTACTCACAC), a wild-type-allele-specific primer located in the UTR (primer a, 5′ CAGGCGTGGTTGCTTTCTTAT), and a mutant-allele-specific primer located at the 3′ end of the neomycin selection cassette (primer b, 5′ AAGCTGATCCGGAACCCTTAAT). PCR was carried out with 25 ng of genomic DNA isolated from tail clippings in 25-μl reaction mixtures containing 1× $MgCl_2$-PCR buffer (QIAGEN), 40 μM of deoxynucleoside triphosphates, 200 μM of each primer, 1× Q solution, and 1.25 U HotStart *Taq* polymerase (QIAGEN). After an initial denaturation at 95°C for 15 min, 35 cycles of PCR at 94°C for 30 s, 58°C for 30 s, and 72°C for 45 s were performed, followed by a final extension at 72°C for 7 min. Amplification of the wild-type and mutant alleles resulted in products of 354 and 184 bp, respectively. DNA extracted from the yolk sac was used to genotype embryonic day 8.5 (E8.5) to E14 embryos. Paraffin sections of E6.5 and E7.5 embryos were subjected to laser microdissection using the Arcturus PixCell laser capture microdissection system according to the supplier's instructions and as described on the National Institutes of Health website (http://dir.nichd.nih.gov/lcm/lcm.htm). DNA was extracted using the Picopure DNA extraction kit (Arcturus) according to the manufacturer's instructions. Genotyping was performed as described above except that 40 cycles of amplification were used. DNA was directly extracted from individual blastocysts by using the Picopure DNA extraction kit (Arcturus) and genotyped as for early embryos.

BrdU labeling and staining. Bromodeoxyuridine (BrdU) (100 μg/g of body weight; BD PharMingen) was injected intraperitoneally into CD-1 mice at 6 weeks of age. Tissues from euthanized mice were dissected 24 h after treatment and were fixed, paraffin embedded, and sectioned as described above. BrdU staining was performed using the BrdU in situ detection kit (BD PharMingen) according to the supplier's recommendations.

Hematological analyses. Mouse peripheral blood cells, including total white count, neutrophils, monocytes, basophils, eosinophils, leukocytes, and red blood cells, were counted using the HEMAVET 950 multispecies hematology system (Drew Scientific, Inc.).

In vitro culture of fibroblasts and blastocysts. Primary fibroblast cultures were established from embryos of heterozygous intercrosses at E15.5 by standard methods (24). DNA was isolated for genotyping, and whole-cell protein extracts were prepared from grown cultures as described above.

Blastocysts were collected by flushing the uteri of pregnant females from *Sbds* heterozygous intercrosses at E3.5 and were individually cultured in 24-well plates in ES cell medium without leukemia-inhibitory factor. The cultures were incubated with 5% CO_2 at 37°C and were examined and photographed every 24 h for up to 4 days. At the end of the observation period, cells were scraped off the dish for DNA extraction and genotyping by PCR as described above.

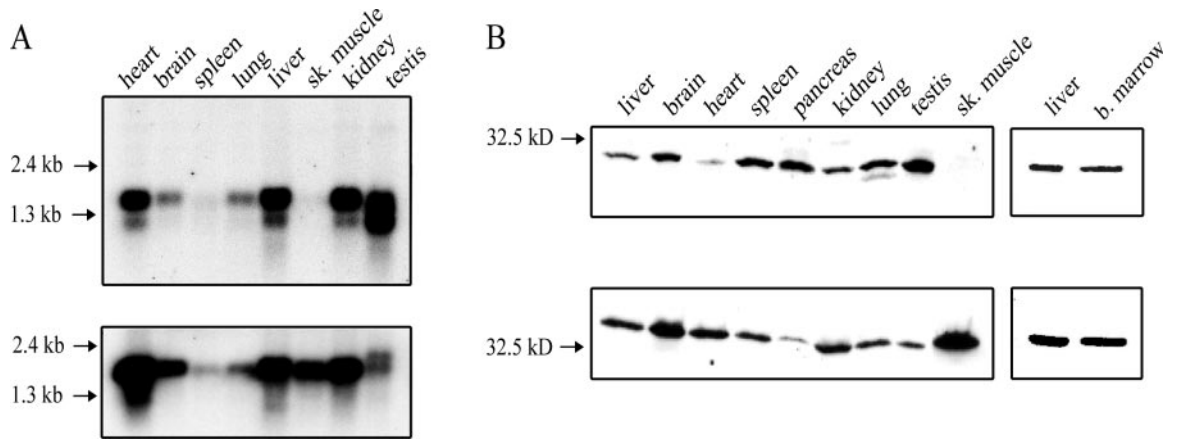

FIG. 1. Expression profiles of *Sbds* mRNA and protein in adult mouse organs. (A) Multitissue Northern blot. Poly(A^+) mRNA of the adult mouse tissues indicated hybridized with *Sbds* (upper panel) and *Gapd* (lower panel) cDNA probes. (B) Multitissue Western blot of mouse tissues with affinity-purified polyclonal anti-SBDS (upper panel) and control anti-mouse Gapd (lower panel) (Abcam) antibodies.

RESULTS

Mouse Sbds and expression profile. Sequence alignment and expressed sequence tag (EST) database analysis revealed a single active mouse ortholog to SBDS. Sbds (Mm.280484) shares 97% identity in protein sequence with SBDS (NP 057122). Similar to the human counterpart, *Sbds* generates a 1.6-kb transcript encoding a protein product with a molecular mass of 29 kDa. We examined expression of Sbds in adult CD-1 mouse tissues by Northern and Western blot analyses (Fig. 1). The analyses revealed a ubiquitous pattern with variable expression levels. High expression is seen in testis, pancreas, lung, spleen, bone marrow, and liver, with the testis having the strongest expression. In contrast, very small amounts of mRNA and protein were detected in heart and skeletal muscle, respectively. The smaller transcript in the Northern analysis (Fig. 1A) that appears most prominent in the testis is likely due to alternative polyadenylation, based on EST entries. This is also supported by observing only single *Sbds* RT-PCR cDNA products from these tissues by using primers located at the 5′ and 3′ ends of the coding region (data not shown), as well as by the absence of any alternative protein isoforms detected by the Western blot analysis (Fig. 1B).

To investigate expression in different cell types, in situ hybridizations were performed on CD-1 mouse tissue sections. *Sbds* expression was detected in most cell types, with very high levels in cells of the bronchiole epithelium in lung (Fig. 2A), small intestine epithelium (Fig. 2B), ovary follicles (Fig. 2C), basal compartment of testis seminiferous tubes (Fig. 2D), and mucosal epithelium of stomach (Fig. 2E). In contrast, relatively low expression is seen in most of the adult brain under comparable hybridization conditions. The cells of the tissues with the highest expression proliferate rapidly compared to their surrounding components. To confirm this, we labeled proliferating cells of CD-1 mice with BrdU (100 μg/g of body weight). When staining patterns were compared to the in situ hybridization signals of adjacent sections, the single BrdU exposure supported that high *Sbds* expression was consistent with rapid cell proliferation (Fig. 2G to O).

The differentiated expression pattern of Sbds in adult mice prompted us to investigate its expression during embryonic development. By EST database analysis, Sbds was found to be expressed in all developmental stages as early as the fertilized egg. In situ hybridization using both whole-mount and section methods confirmed the ubiquitous but variable expression levels in different tissues of the embryo (see Fig. S2 in the supplemental material). Northern blot analysis using mRNA from whole embryos showed that the *Sbds* transcript level is initially very high but that it subsequently decreases from early to mid- and late embryonic stages (Fig. 3). This was also apparent using in situ hybridization with CD-1 mouse embryos controlled for consistent reaction conditions (see Fig. S3 in the supplemental material). Overall, *Sbds* expression decreases from early to later stages of the embryo in parallel with growth rate changes.

In summary, Sbds was found to be ubiquitously expressed in all embryonic stages and most adult tissues. In addition, its elevated expression in rapidly growing tissues may highlight a critical aspect of function required for cell proliferation.

Targeted disruption of the *Sbds* gene. To investigate the role of Sbds in vivo, we generated a null allele through gene targeting technology (Fig. 4). The *Sbds* genomic sequence was isolated from a 129S6/SvEvTac mouse BAC library and subsequently inserted into the targeting vector. The *Sbds* null allele was achieved with the interruption of translation in exon 1 through the insertion of an *IRES-lacZ* and neomycin resistance cassette. A diphtheria toxin A gene was also included in the vector to provide negative selection of ES cells that did not undergo homologous recombination (Fig. 4A). Linearized vector DNA was electroporated into W4 ES cells. Twenty-four percent of neomycin resistance clones were identified as having the desired recombination by Southern blot analysis with 5′ and 3′ external probes (Fig. 4B). Two independently derived $Sbds^{+/-}$ ES clones were microinjected into C57BL/J6 blastocysts to establish mutant allele strains. Germ line transmission was evaluated by PCR genotyping (Fig. 4C). The targeted alleles were maintained in hybrid C57BL/6J and 129S6/SvEvTac genetic backgrounds, and the two lines led to the generation of mice with identical phenotypes, as described below.

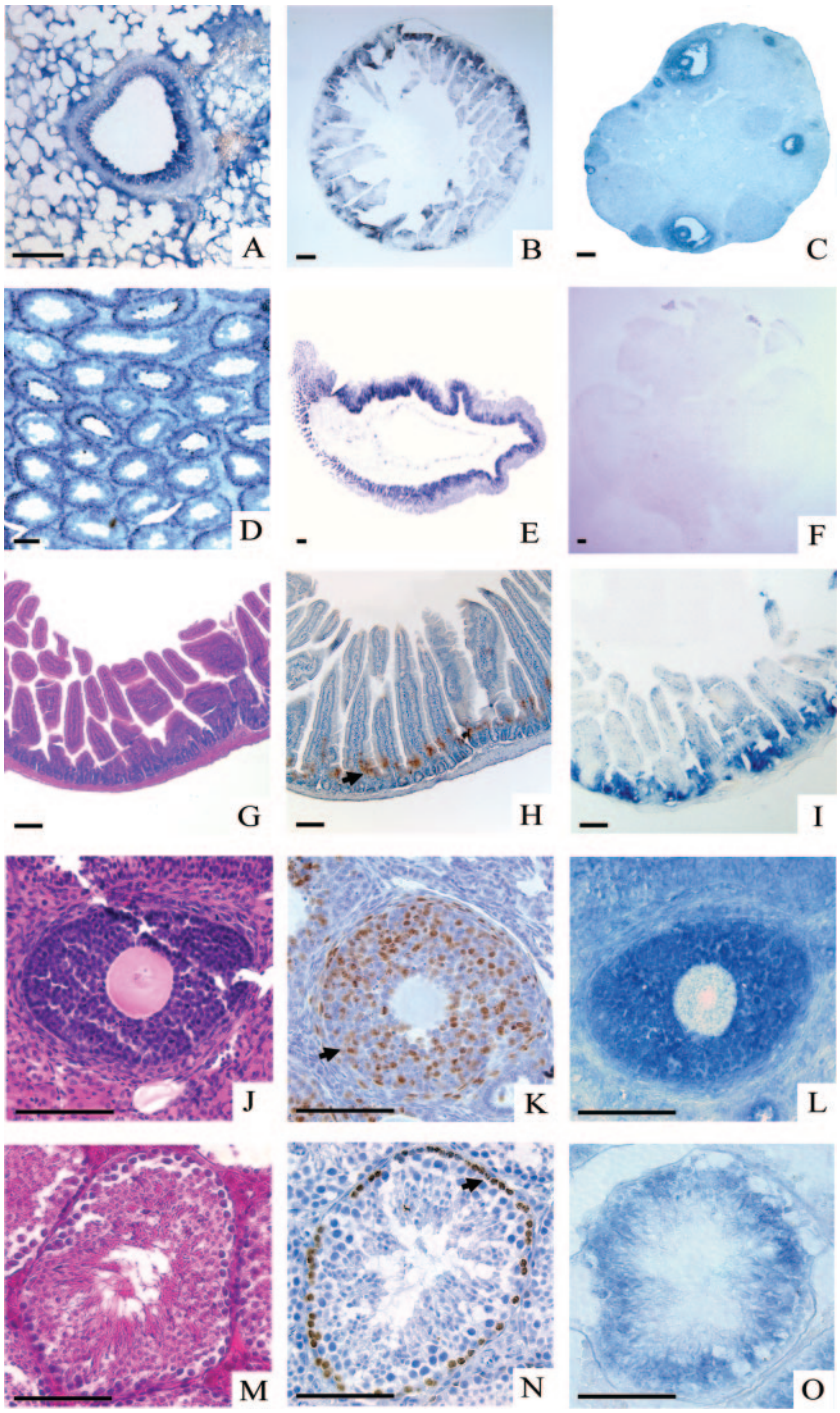

FIG. 2. *Sbds* is highly expressed in rapidly proliferating tissues. In situ hybridization with a *Sbds* cDNA probe is shown. High expression was found in bronchiole epithelium in lung (A), small intestine epithelium (B), ovary follicles (C), testis seminiferous tube (D), and mucosal epithelium of stomach (E). In contrast, the expression in adult brain (F) is low. Increased *Sbds* expression was correlated with rapidly proliferating cells in small intestine epithelium (G, H, and I), ovary follicles (J, K, and L) and testis seminiferous tubes (M, N, and O). (G, J, and M) Hematoxylin and eosin staining of intestine epithelium, ovary follicles, and testis seminiferous tubes, respectively. (I, L, and O) In situ hybridization of adjacent tissue sections, respectively, with a cDNA probe consisting of the 5′ UTR and exons 1 to 3 of *Sbds*. (H, K, and N) Adjacent sections, respectively, were stained with an anti-BrdU antibody. Arrows mark examples of cells with incorporation of BrdU. Bars, 100 μm.

Consistent with the targeting of the *Sbds* locus, Western blot analysis of protein extracts from embryonic fibroblast cells of heterozygous mice showed reduced levels (approximately 50%) of Sbds compared to extracts from wild-type littermates (Fig. 4D). Heterozygous mice ($Sbds^{+/-}$) were fertile and developed normally. Cohorts of heterozygous mice were kept for up to 18 months and showed no predisposition to ill health compared with age- and sex-matched wild-type littermates.

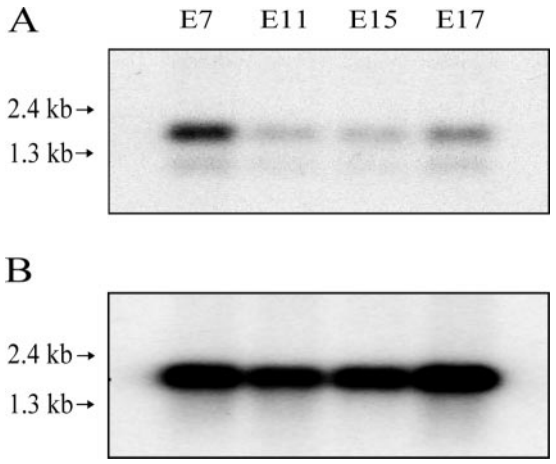

FIG. 3. Expression of *Sbds* during mouse embryonic development. (A and B) Mouse embryo multiple-tissue Northern blot. Poly(A^+) mRNA from whole mouse embryo at the stages indicated was hybridized with *Sbds* cDNA (A) and *Gapd* cDNA (B) probes.

Specifically, we examined the growth rate (body weight and body length), blood cell counts (neutrophils, red blood cells, leukocytes, and platelets), and bone development (bone staining). No SDS-related phenotypes were found in the heterozygous mice (data not shown).

TABLE 1. Genotype and phenotype analysis of embryos and offspring from $Sbds^{+/-}$ intercrosses[a]

Stage	No. of embryos[b]				
	With genotype:			With empty deciduae	Total
	$Sbds^{+/+}$	$Sbds^{+/-}$	$Sbds^{-/-}$		
E3.5	9	17	8		34
E6.5	6	15	4 (4)	0	25 (4)
E7.5	5	23	7 (7)	0	35 (7)
E8.5	16	19	8 (8)	0	43 (8)
E9.5	4	12	0	4	20
E10.5	9	16	0	9	34
Full term	39	74	0		113

[a] Live-born offspring, staged embryos (E6.5 to E10.5), and blastocysts (E3.5) were genotyped by PCR.
[b] The number of phenotypically abnormal embryos is indicated in parentheses.

Sbds deficiency causes early embryonic lethality. $Sbds^{+/-}$ mice were intercrossed to evaluate the phenotype of $Sbds^{-/-}$ animals. Genotyping of 113 offspring from 20 litters revealed that 39 were wild type ($Sbds^{+/+}$) and 74 were heterozygous

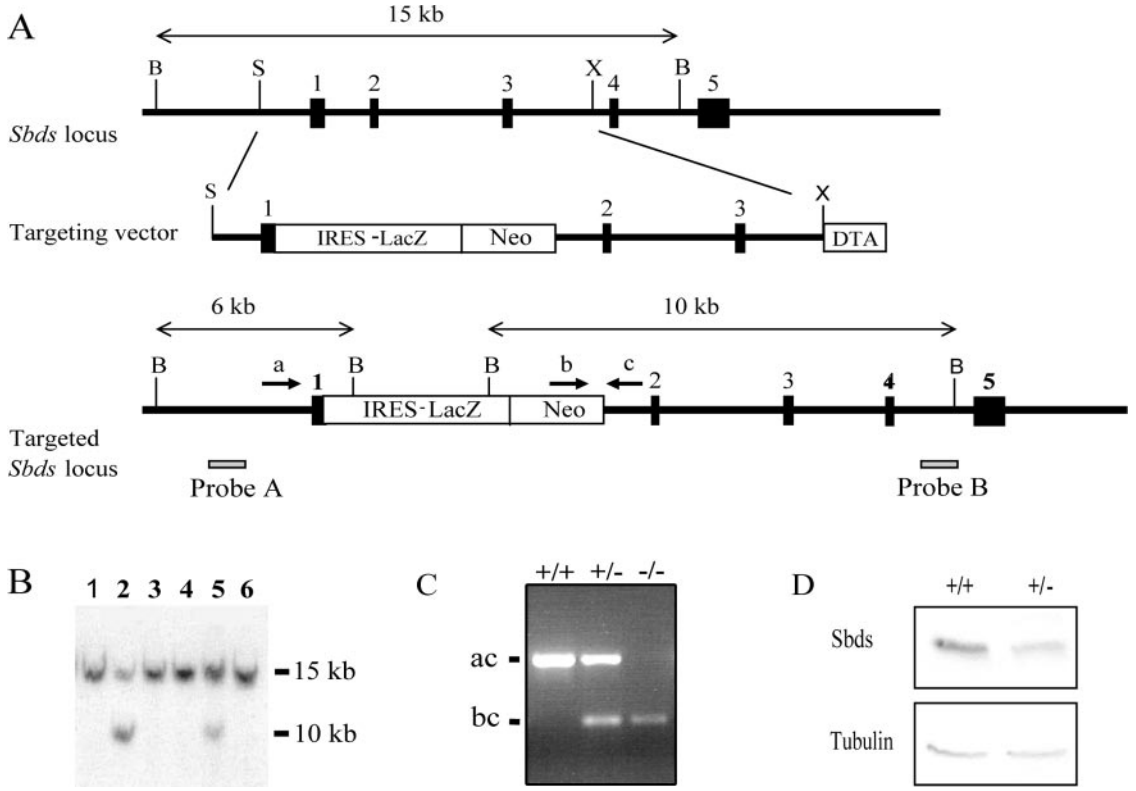

FIG. 4. Targeted disruption of the mouse *Sbds* gene. (A) Genomic organization of the mouse *Sbds* gene. The targeting vector and the desired homologous recombination outcome are illustrated. Black boxes represent *Sbds* exons. Probes A and B correspond to 5′ and 3′ external probes used for Southern blot-based genotyping; arrows a, b, and c correspond to oligonucleotide primers for PCR genotyping. Relevant restriction sites are BamHI (B), BssSI (S), and XbaI (X). (B) Representative Southern blot analysis of neomycin-resistant ES cells. Genomic DNA was digested with BamHI and hybridized with probe B. The 15-kb and 10-kb bands represent the wild-type (lanes 1, 3, 4, and 6) and targeted (lanes 2 and 5) alleles, respectively. (C) Representative PCR genotyping with primers a, b, and c. The observed PCR products derived from wild-type (+) and targeted (−) alleles are 354 and 184 bp, respectively. (D) Sbds expression was evaluated in wild-type and heterozygous embryonic fibroblasts by Western blotting using the anti-SBDS antibody (upper panel), with comparison to α-tubulin as a control for loading as detected by anti-α-tubulin antibody (lower panel) (Molecular Probes).

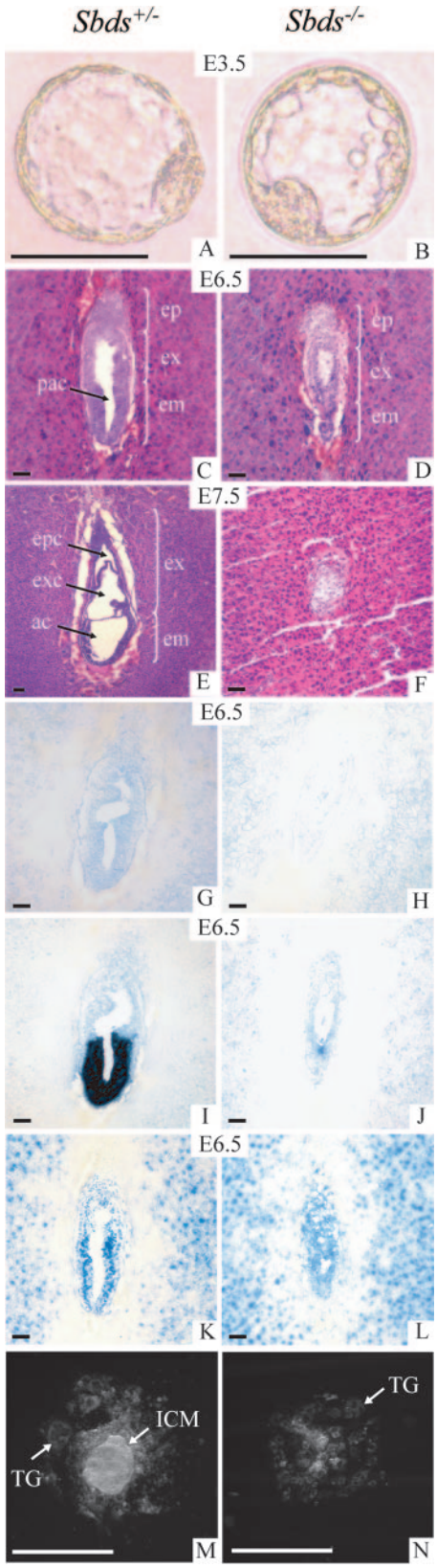

FIG. 5. Failed development of *Sbds*$^{-/-}$ embryos. (A and B) *Sbds*$^{+/-}$ (A) and *Sbds*$^{-/-}$ (B) blastocysts at E3.5 appear normal. (C to F) Sagittal sections of hematoxylin- and eosin-stained *Sbds*$^{+/-}$ (C and E) and *Sbds*$^{-/-}$ (D and F) embryos at E6.5 and E7.5; disorganization of the null embryo was apparent at E6.5 (D), with subsequent degradation clearly evident by E7.5 (F). (G to L) In situ hybridization of *Sbds* cDNA with exons 3 and 4 and *Oct4* cDNA and *Bmp4* cDNA probes on heterozygous (G, I, and K) and null (H, J, and L) E6.5 embryos. (M and N) *Sbds*$^{+/-}$ blastocysts (M) were able to outgrow after 4 days of culture. The growing ICM cells are surrounded by trophoblast giant cells (TG). By contrast, *Sbds*$^{-/-}$ blastocysts (N) retain trophoblast cells but no ICM growth. ac, amniotic cavity; ep, ectoplacental cone; em, embryonic portion; ex, extraembryonic portion; exc, exocoelom; pac, proamniotic cavity. Bars, 50 μm (A, B, M, and N) and 100 μm (C to L).

(*Sbds*$^{+/-}$) for the targeted allele. The complete absence of homozygous (*Sbds*$^{-/-}$) offspring, the observed ratio of the wild-type and heterozygous progeny, and the small litter size (mean of 5.7, compared to 8.4 for heterozygote and wild-type mouse crosses) suggested that ablation of Sbds led to embryonic lethality.

To determine the stage of lethality, E3.5 blastocysts from *Sbds*$^{+/-}$ intercrosses were isolated and genotyped. Among a total of 34 blastocysts from three matings, 9 (26%) were *Sbds*$^{+/+}$, 17 (50%) were *Sbds*$^{+/-}$, and 8 (24%) were *Sbds*$^{-/-}$ (Table 1). The morphology of the *Sbds*$^{-/-}$ blastocysts was indistinguishable from those of the *Sbds*$^{+/-}$ and *Sbds*$^{+/+}$ blastocysts in terms of their appearance and the size of the inner cell mass (ICM) (Fig. 5A and B), indicating that the ablation does not affect development prior to implantation. We then analyzed early postimplantation stages with histological sections. At E6.5, analysis of 25 embryos from three pregnancies revealed 6 (25%) *Sbds*$^{+/+}$, 15 (63%) *Sbds*$^{+/-}$, and 4 (17%) *Sbds*$^{-/-}$ embryos. The *Sbds*$^{-/-}$ embryos were approximately two-thirds of the size of the *Sbds*$^{+/-}$ embryos. The ectoplacental cone and extraembryonic portions of the *Sbds*$^{-/-}$ embryos, although smaller, were morphologically comparable to those of their heterozygous littermates (Fig. 5C and D). Although two-layered egg cylinders were apparent, the embryonic portion of the *Sbds*$^{-/-}$embryos was much smaller than that of the *Sbds*$^{+/-}$ embryos. Also, proaminotic cavities in the embryonic portions of the *Sbds*$^{-/-}$ embryos were not visible. At E7.5, while all wild-type and heterozygous embryos examined had gastrulated and developed a third germ layer (mesoderm), the *Sbds*$^{-/-}$ embryos had not developed past the egg cylinder stage and had not undergone gastrulation. They were significantly smaller and appeared to be undergoing degradation. Eight *Sbds*$^{-/-}$ embryos were found from 43 embryos at E8.5, but all were almost completely resorbed, and only empty deciduae were evident by the later stages of E9.5 and E10.5. Therefore, *Sbds*$^{-/-}$ mutant embryos displayed severe growth and morphological defects by the onset of gastrulation and ceased to develop prior to E6.5.

Sbds is required for early embryo development. To confirm that Sbds was ablated in the *Sbds*$^{-/-}$ embryo, the mRNA level was analyzed by in situ hybridization using a *Sbds* cDNA probe containing exons 3 and 4 only. No *Sbds* transcript was detected in the E6.5 null embryos compared with their heterozygous littermates (Fig. 5G and H).

To investigate the developmental defect in the E6.5 *Sbds*$^{-/-}$ embryos, we performed in situ hybridization using an *Oct4* cDNA probe as a marker for embryonic stem cells and the

TABLE 2. Genotype and phenotype analysis of cultured Sbds blastocysts

Genotype	Total no. of blastocysts	No. (%) with ICM outgrowth:	
		Normal	Abnormal[a]
Sbds$^{+/+}$	10	9 (90)	1 (10)
Sbds$^{+/-}$	13	11 (85)	2 (15)
Sbds$^{-/-}$	6	0 (0)	6 (100)

[a] Blastocysts with failed ICM outgrowth.

epiblast. In *Sbds*$^{+/-}$ embryos, the inner layer of the embryonic portion showed intense hybridization, indicating the growth and development of the epiblast (Fig. 5I). In contrast *Oct4*-positive cells were rare in the *Sbds*$^{-/-}$ embryos (Fig. 5J). Examination by in situ hybridization with a *Bmp4* cDNA probe to mark extraembryonic tissue (Fig. 5K and L) and a cDNA probe containing the 5′ UTR and exons 1 through 3 of *Sbds* (data not shown) revealed that the extraembryonic tissue of the E6.5 *Sbds*$^{-/-}$ embryo was able to develop.

To directly determine the growth capability of *Sbds*$^{-/-}$ embryos, blastocysts at E3.5 from timed heterozygous matings were collected and individually cultured in vitro. After 1 day, all isolated blastocysts hatched from the zona pellucida, adhered to the tissue culture plastic, and began to grow out. After 4 days in culture, *Sbds*$^{-/-}$ embryos (Fig. 5N) exhibited giant cell trophoblasts comparable to those of their heterozygote (Fig. 5 M) or wild-type (data not shown) littermates. However, the ICM components did not grow for any of the *Sbds*$^{-/-}$ blastocysts (6/6) (Table 2), in contrast to only 15% of *Sbds*$^{+/-}$ (2/13) and 10% of *Sbds*$^{+/+}$ (1/10) blastocysts (representative outgrowth examples are shown in Fig. 5M and N). In addition, we also attempted to generate homozygous *Sbds*-targeted ES cells. A total of 1×10^8 heterozygous targeted ES cells were cultured in ES cell medium with a range of high doses of G418 (0.75 mg/ml to 6 mg/ml) in order to select for rare homozygous targeted clones (22). A total of 130 clones resistant to high levels of neomycin were generated; however, PCR genotyping revealed that none were homozygously targeted for the *Sbds* gene (data not shown). These results suggested that Sbds function is essential for the viability and/or proliferation of early embryonic tissue.

In summary, we found that that *Sbds*$^{+/-}$ mice have normal phenotypes, indistinguishable from those of their wild-type littermates. However, the development of *Sbds*$^{-/-}$ embryos was arrested earlier than E6.5, leading to early lethality with markedly muted epiblast development from the inner cell mass tissue. Therefore, *Sbds* is an essential gene for early mouse development.

DISCUSSION

SDS is a recessive disorder resulting from the loss of SBDS function. In this study we found that *Sbds* is an essential gene in mouse, consistent with observations of SBDS mutations in SDS patients. Analysis of our large patient collection has revealed two common SBDS mutations, the first, a stop codon (183-184TA→CT) in exon 2 and the second a splice donor mutation (258-2T→C) in intron 2. These mutations can be found with other rare mutations, but many patients are heterozygous for these common changes (5). Interestingly, while some patients are homozygous for the splice donor mutation, no patients (of over 250 families) are homozygous for the early truncation mutation. This correlates with the findings of the mouse model, where the combination of two null *Sbds* alleles is not compatible with life. We also found that the mice that are heterozygous for one null allele have normal growth phenotypes and exhibit no apparent skeleton abnormalities or hematopoietic or exocrine pancreatic dysfunction, consistent with the absence of disease phenotypes in SDS carriers. It is therefore evident that many disease alleles lead to loss of function but that patients likely have low residual SBDS activity.

A recent study revealed the localization of SBDS in normal human fibroblasts, with its apparent concentration in the nucleolus, where rRNA and ribosomes mature (3). There is cell cycle dependence, with nucleolar localization during the G_1 and G_2 cell phases and more diffuse nuclear localization during S phase. High expression during rapid growth and proliferation aligns well with a role of Sbds in rRNA metabolism and ribosome biogenesis and with the localization studies. Marked increases in de novo protein synthesis and RNA metabolism are especially essential after implantation. As the function of Sbds has not been elucidated, it is difficult to precisely target the inadequacy that leads to ICM and epiblast demise, possibly due to low Sbds directly or to the specific loss of a downstream metabolite requirement. Our observations, taken together with consideration of a possible long half-life (on the order of hours) and the very low level of SBDS observed in patients (3; unpublished observations), indicate that a maternal protein effect may be enabling survival to beyond the implantation period.

A large number of gene ablations with the timing of lethality comparable to that for Sbds have been described (7). Also relevant, for comparison, are those genes affected in other human syndromes involving deficiency in RNA and/or ribosome metabolism with similarity in clinical features of hematological deficiency and leukemia susceptibility. The congenital bone marrow failure syndrome Diamond-Blackfan anemia is one such syndrome, frequently resulting from loss of RPS19, a ribosomal component. However, and in contrast to the case for Sbds, its ablation leads to lethality very early, prior to implantation (20). Another bone marrow failure syndrome, dyskeratosis congenita, can be caused by mutations in different genes, one being *DKC1* (encoding dyskerin) on the X chromosome. Ablation of dyskerin in male mice leads to apparent abnormality as early as E7.5 with subsequent embryo resorption (11). While dyskerin does localize to the nucleolus as well as the nucleoplasm, consistent with its predicted role in rRNA processing, interpretation of phenotype must also consider dyskerin's apparent role in telomere function (12). Direct comparison to loss of Sbds is limited pending more information on the function or functions of the genes involved in these syndromes.

SBDS protein family members are highly conserved. Taken together with the observed ubiquitous and essential expression, it is apparent that Sbds plays an important role in the cells of many tissues. Given the clinical picture of SDS patients, which includes overt symptoms in only some tissues and in some cell types, it would also appear that there is variable sensitivity to the loss of SBDS function. The occurrence of symptoms does not directly correlate with tissue levels of mRNA (in human [5] or mouse [this study]). For example, the exocrine components

constitute the bulk of pancreatic tissue that exhibits relatively high levels of Sbds expression, and yet this compartment is extremely sensitive to SBDS loss in patients. Pancreatic exocrine dysfunction is a universal feature of patients with SBDS mutations (14; unpublished observations). Bone marrow exhibits relatively lower expression. Although microarray analysis has shown that SBDS expression is high in human hematopoietic stem cell and progenitor cell populations compared to mature blood cell populations (John Dick, personal communication), deficiencies of the mature neutrophils, in both their abilities and numbers, are the most common hematological deficiencies observed in SDS (10). An essential gene can lead to differential outcomes if tissues have different requirements for the gene product, either constitutively or at specific developmental stages. Alternatively, it may also be that loss may be compensated in a tissue- or cell type-specific manner. The sensitivity of loss of Sbds in the severely afflicted tissues requires further investigation to distinguish between these possibilities.

In this study, we have found that Sbds is ubiquitously expressed in all stages of mouse embryonic development and in adult tissues, with levels that are generally correlated with cell proliferation. As *Sbds* was also found to be essential in mice, hypomorphic or conditional alleles in combination with the generated null allele will be required to provide disease-relevant mouse models for the detailed study of SDS pathogenesis. These mammalian models can be used to investigate which, and how, processes are affected in the organs that exhibit the most severe clinical phenotypes when thresholds of SBDS reach critically low levels. They will also provide insight into why only specific organs show effects and how variability in presentation of disease ensues.

ACKNOWLEDGMENTS

We thank D. Sinasac and A. Nagy for advice on the generation of the mouse model, J. Rossant and P. Georgiades for advice and probes for the analysis of early embryos, and N. Richards and G. R. B. Boocock for generating and evaluating the anti-SBDS antibody.

This work was supported by grants MT-15074 from the Canadian Institutes of Health Research (CIHR) and HL79573 from the National Institutes of Health. S.Z. is a recipient of a studentship from the CIHR-University of Toronto Training Program in Molecular Medicine. J.M.R. is a member of the Canadian Genetic Diseases Network.

REFERENCES

1. **Aggett, P. J., N. P. Cavanagh, D. J. Matthew, J. R. Pincott, J. Sutcliffe, and J. T. Harries.** 1980. Shwachman's syndrome. A review of 21 cases. Arch. Dis. Child. **55:**331–347.
2. **Aggett, P. J., J. T. Harries, B. A. Harvey, and J. F. Soothill.** 1979. An inherited defect of neutrophil mobility in Shwachman syndrome. J. Pediatr. **94:**391–394.
3. **Austin, K. M., R. J. Leary, and A. Shimamura.** 2005. The Shwachman-Diamond SBDS protein localizes to the nucleolus. Blood **106:**1253–1258.
4. **Bodian, M., W. Sheldon, and R. Lightwood.** 1964. Congenital hypoplasia of the exocrine pancreas. Acta Paediatr. **53:**282–293.
5. **Boocock, G. R., J. A. Morrison, M. Popovic, N. Richards, L. Ellis, P. R. Durie, and J. M. Rommens.** 2003. Mutations in SBDS are associated with Shwachman-Diamond syndrome. Nat. Genet. **33:**97–101.
6. **Boocock, G. R., M. R. Marit, and J. M. Rommens.** 2006. Phylogeny, sequence conservation, and functional complementation of the SBDS protein family. Genomics **87:**758–771
7. **Copp, A. J.** 1995. Death before birth: clues from gene knockouts and mutations. Trends Genet. **11:**87–93.
8. **Dokal, I., S. Rule, F. Chen, M. Potter, and J. Goldman.** 1997. Adult onset of acute myeloid leukaemia (M6) in patients with Shwachman-Diamond syndrome. Br. J. Haematol. **99:**171–173.
9. **Dror, Y., H. Ginzberg, I. Dalal, V. Cherepanov, G. Downey, P. Durie, C. M. Roifman, and M. H. Freedman.** 2001. Immune function in patients with Shwachman-Diamond syndrome. Br. J. Haematol. **114:**712–717.
10. **Ginzberg, H., J. Shin, L. Ellis, J. Morrison, W. Ip, Y. Dror, M. Freedman, L. A. Heitlinger, M. A. Belt, M. Corey, J. M. Rommens, and P. R. Durie.** 1999. Shwachman syndrome: phenotypic manifestations of sibling sets and isolated cases in a large patient cohort are similar. J. Pediatr. **135:**81–88.
11. **He, J., S. Navarrete, M. Jasinski, T. Vulliamy, I. Dokal, M. Bessler, and P. J. Mason.** 2002. Targeted disruption of Dkc1, the gene mutated in X-linked dyskeratosis congenita, causes embryonic lethality in mice. Oncogene **21:**7740–7744.
12. **Heiss, N. S., A. Girod, R. Salowsky, S. Wiemann, R. Pepperkok, and A. Poustka.** 1999. Dyskerin localizes to the nucleolus and its mislocalization is unlikely to play a role in the pathogenesis of dyskeratosis congenita. Hum. Mol. Genet. **8:**2515–2524.
13. **Hill, R. E., P. R. Durie, K. J. Gaskin, G. P. Davidson, and G. G. Forstner.** 1982. Steatorrhea and pancreatic insufficiency in Shwachman syndrome. Gastroenterology **83:**22–27.
14. **Ip, W. F., A. Dupuis, L. Ellis, S. Beharry, J. Morrison, M. O. Stormon, M. Corey, J. M. Rommens, and P. R. Durie.** 2002. Serum pancreatic enzymes define the pancreatic phenotype in patients with Shwachman-Diamond syndrome. J. Pediatr. **141:**259–265.
15. **Kent, A., G. H. Murphy, and P. Milla.** 1990. Psychological characteristics of children with Shwachman syndrome. Arch. Dis. Child. **65:**1349–1352.
16. **Koonin, E. V., Y. I. Wolf, and L. Aravind.** 2001. Prediction of the archaeal exosome and its connections with the proteasome and the translation and transcription machineries by a comparative-genomic approach. Genome Res. **11:**240–252.
17. **Liebman, W. M., E. Rosental, M. Hirshberger, and M. M. Thaler.** 1979. Shwachman-Diamond sydnrome and chronic liver disease. Clin. Pediatr. (Philadelphia) **18:**695–698.
18. **Mack, D. R., G. G. Forstner, M. Wilschanski, M. H. Freedman, and P. R. Durie.** 1996. Shwachman syndrome: exocrine pancreatic dysfunction and variable phenotypic expression. Gastroenterology **111:**1593–1602.
19. **Makitie, O., L. Ellis, P. R. Durie, J. A. Morrison, E. B. Sochett, J. M. Rommens, and W. G. Cole.** 2004. Skeletal phenotype in patients with Shwachman-Diamond syndrome and mutations in SBDS. Clin. Genet. **65:**101–112.
20. **Matsson, H., E. J. Davey, N. Draptchinskaia, I. Hamaguchi, A. Ooka, P. Leveen, E. Forsberg, S. Karlsson, and N. Dahl.** 2004. Targeted disruption of the ribosomal protein S19 gene is lethal prior to implantation. Mol. Cell. Biol. **24:**4032–4037.
21. **Mo, R., A. M. Freer, D. L. Zinyk, M. A. Crackower, J. Michaud, H. H. Heng, K. W. Chik, X. M. Shi, L. C. Tsui, S. H. Cheng, A. L. Joyner, and C. Hui.** 1997. Specific and redundant functions of Gli2 and Gli3 zinc finger genes in skeletal patterning and development. Development **124:**113–123.
22. **Mortensen, R. M., D. A. Conner, S. Chao, A. A. Geisterfer-Lowrance, and J. G. Seidman.** 1992. Production of homozygous mutant ES cells with a single targeting construct. Mol. Cell. Biol. **12:**2391–2395.
23. **Motoyama, J., J. Liu, R. Mo, Q. Ding, M. Post, and C. C. Hui.** 1998. Essential function of Gli2 and Gli3 in the formation of lung, trachea and oesophagus. Nat. Genet. **20:**54–57.
24. **Nagy, A., Gersenstein, M., Vintersten, K.** 2002. Manipulating the mouse embryo: a laboratory manual, 3rd ed. Cold Spring Harbor Laboratory Press, Cold Spring Harbor, N.Y.
25. **Peng, W. T., M. D. Robinson, S. Mnaimneh, N. J. Krogan, G. Cagney, Q. Morris, A. P. Davierwala, J. Grigull, X. Yang, W. Zhang, N. Mitsakakis, O. W. Ryan, N. Datta, V. Jojic, C. Pal, V. Canadien, D. Richards, B. Beattie, L. F. Wu, S. J. Altschuler, S. Roweis, B. J. Frey, A. Emili, J. F. Greenblatt, and T. R. Hughes.** 2003. A panoramic view of yeast noncoding RNA processing. Cell **113:**919–933.
26. **Sambrook, J., Russell, and D. W.** 2001. Molecular cloning: a laboratory manual, 3rd ed. Cold Spring Harbor Laboratory Press, Cold Spring Harbor, N.Y.
27. **Savchenko, A., N. Krogan, J. R. Cort, E. Evdokimova, J. M. Lew, A. A. Yee, L. Sanchez-Pulido, M. A. Andrade, A. Bochkarev, J. D. Watson, M. A. Kennedy, J. Greenblatt, T. Hughes, C. H. Arrowsmith, J. M. Rommens, and A. M. Edwards.** 2005. The Shwachman-Bodian-Diamond syndrome protein family is involved in RNA metabolism. J. Biol. Chem. **280:**19213–19220.
28. **Shammas, C., T. F. Menne, C. Hilcenko, S. R. Michell, B. Goyenechea, G. R. Boocock, P. R. Durie, J. M. Rommens, and A. J. Warren.** 2005. Structural and mutational analysis of the SBDS protein family: insight into the leukemia-associated Shwachman-Diamond syndrome. J. Biol. Chem. **280:**19221–19229.
29. **Shwachman, H., L. K. Diamond, F. A. Oski, and K. T. Khaw.** 1964. The syndrome of pancreatic insufficiency and bone marrow dysfunction. J. Pediatr. **65:**645–663.
30. **Smith, O. P., I. M. Hann, J. M. Chessells, B. R. Reeves, and P. Milla.** 1996. Haematological abnormalities in Shwachman-Diamond syndrome. Br. J. Haematol. **94:**279–284.
31. **Stepanovic, V., D. Wessels, F. D. Goldman, J. Geiger, and D. R. Soll.** 2004. The chemotaxis defect of Shwachman-Diamond syndrome leukocytes. Cell Motil. Cytoskel. **57:**158–174.
32. **Woods, W. G., J. S. Roloff, J. N. Lukens, and W. Krivit.** 1981. The occurrence of leukemia in patients with the Shwachman syndrome. J. Pediatr. **99:**425–428.
33. **Wu, L. F., T. R. Hughes, A. P. Davierwala, M. D. Robinson, R. Stoughton, and S. J. Altschuler.** 2002. Large-scale prediction of Saccharomyces cerevisiae gene function using overlapping transcriptional clusters. Nat. Genet. **31:**255–265.